Heliyon 10 (2024) e32941

Contents lists available at ScienceDirect

Heliyon

journal homepage: www.cell.com/heliyon

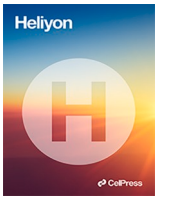

Research article

Multi-variate multi-objective optimization of production conditions for electro-spun skin scaffold using RSM and investigation of gamma irradiation effects on the properties of the optimized sample

M. Hoseini [a,*], S. Hamidi [a], E. Salehi [b], A. Mohammadi [a], F. Mirhoseini [c], M. Ravaghi [a]

[a] Department of Physics, Faculty of Science, Arak University, P.O. Box: 38156, Arak, Iran
[b] Chemical Engineering Department, Faculty of Engineering, Arak University, P.O. Box: 38156, Arak, Iran
[c] Department of Chemistry, Faculty of Science, Arak University, P.O. Box: 38156, Arak, Iran

ARTICLE INFO

Keywords:
Multi-variate multi-objective optimization
Response surface methodology
Polycaprolactone nanofiber
Skin scaffold
Design expert
Sobol sensitivity analysis
Gamma-ray sterilization

ABSTRACT

Developing electro-spun scaffolds with ideal mechanical properties for skin purposes can profit from using the Response Surface Methodology technique to define and optimize the outcome quality and required sterilization for use in vivo. This study investigated the effects of four main independent electrospinning variables for polycaprolactone nanofibers scaffold using multi-variable and multi-objective optimization. It was done to determine significant parameters on responses and find optimal conditions to reach the preferred properties. Young's modulus, elongation-at-break, and tensile strength were the responses. After obtaining appropriate models, the impact share of variables on the responses was determined using Sobol sensitivity analysis. The results showed that flow rate is the most significant parameter of elastic modulus and tensile strength responses, with 76.45 % and 41.27 % impact shares, respectively. The polymer concentration is the following significant parameter on elongation at break, tensile strength and, Young's modulus responses with 64.35 %, 39.485 and, 14.28 % impact share, respectively. Based on the optimized results, a skin scaffold with desired mechanical properties was achieved (under solution concentration of 10 % w/v, flow rate of 2 mL/h, nuzzle-collector distance of 15 cm, and applied voltage of 20 kV). Then it was sterilized with gamma radiation of various doses (25, 40, and 55 kGy) to use in vivo. The SEM analysis indicated no significant change in fibrous morphology due to gamma irradiation at any dosage. FTIR analysis demonstrated the breakup of ester bonds due to gamma irradiation. For samples irradiated by 25 kGy, the crystallinity percentage decreased and chains crosslinking without losing the mechanical stability was dominant. The studies demonstrated that 25 kGy of gamma irradiation could improve the mechanical properties of the optimized PCL skin scaffold, which is very promising for wound healing.

Abbreviation List

(*continued on next page*)

* Corresponding author.
E-mail address: Hosseini.Mahsa2011@gmail.com (M. Hoseini).

https://doi.org/10.1016/j.heliyon.2024.e32941
Received 2 February 2024; Received in revised form 11 June 2024; Accepted 12 June 2024
Available online 18 June 2024

(*continued*)

Abbreviation List	
Response Surface Methodology	RSM
Polycaprolactone	PCL
Scanning Electron Microscopy	SEM
Fourier-transform Infrared Spectroscopy	FTIR
X-Ray Diffraction Analysis	XRD

1. Introduction

Tissue engineering involves using one-dimensional nanostructured materials as a fibrous structure called scaffold for tissue repair and reconstruction that provides the conditions for the diffusion of vital cell nutrients [1–3].

Electrospinning is the most popular method because of its easiness and affordability among the different techniques available for casting nanofiber scaffolds. It allows for the production of nanofibers made from complex components and for various applications [2, 4–11].

One of the most widely studied polymers in tissue engineering for preparing scaffolds is polycaprolactone (PCL). PCL is a synthetic biodegradable, biocompatible, water resistant, nontoxic, and inexpensive polymer that makes it a potential alternative for utilization in biomedical applications [2,3,5–7,10,12–14]. A perfect electro-spun nanofibrous scaffold for biomedical applications should have adequate mechanical adoption with the surrounding tissue. It should have a pattern for tissue growth and helps cell growth, proliferation, and differentiation [2,7]. It has been proven that the strength and deformability of nanofibers impact vitro cell migration, duplication, and discrimination, along with cell morphology [7]. Electro-spun process parameters such as electrical potential field, flow rate, polymer concentration, and the distance between the nozzle and the collector affect the structural properties of the nanofiber scaffolds [3]. Some studies have reported the relationship between the mechanical properties of scaffolds and these operational parameters. Some of these studies have only been focused on the effect of one of these parameters, such as polymer concentration or electrical potential field, on the PCL scaffold mechanical strength [2,8]. Other studies applied the Response Surface Methodology (RSM) and investigated the effects of all or some of the mentioned parameters or other affecting parameters like temperature. They optimize the conditions for synthesizing the PCL scaffolds with preferred properties such as the diameter of nanofibers, tensile strength, and elastic modulus [15–17]. Anindayajati et al. reported that flow rate and polymer concentration have positive effects while increasing the applied voltage and nuzzle-collector distance has a negative impact on Young's modulus [17]. In addition, the non-significance of the nuzzle-collector distance effect on the tensile strength was also uncovered by the researchers [15].

The skin scaffolds must have mechanical properties comparable to the native tissue [11]. The Young's modulus indicates the stress level required to deform the material. On the other hand, tensile strength shows the maximum stress that can be sustained before the material failure. Also, elongation at break is often considered to estimate ductility [18]. According to the literature, Young's modulus between 4.5 and 20 MPa [19,20], tensile strength between 2 and 16 MPa, and the elongation-at-break between 70 and 77 % [20,21], are favored for skin wound dressings purposes. To achieve a nanofiber scaffold with ideal mechanical properties during the electro-spun process, it should consider the effects of all the process variables simultaneously.

For clinical operations, one of the essential features of the scaffolds is to be sterilized. Several sterilization methods containing peracetic acid (PAA), ethylene oxide, dry heat, plasma, and different types of radiation, such as electron beam radiation, X-ray, and gamma-ray sterilization methods, have been investigated over the past decades [22,23]. The sterilization method has to be selected relevant to the material properties because sterilization itself may be unsuitable, ineffectual, or even destructive. Because scaffolds usually have porous structures, a sterilization method is needed to penetrate the materials network without leaving side residues that affect the capacity of cell attachment and growth capacity [13,14,22,24]. Gamma irradiation is highly penetrative leaving no residues in the texture. It induces damage to the molecular level of the electro-spun polymeric scaffold, leading to the death of microorganisms [13,14,22]. In general, gamma radiation can lead to the breaking of polymer chains, resulting in reduced molecular weight or crosslinking of polymer chains with the formation of large three-dimensional networks and increasing the molecular weight of the polymer [25]. During irradiation, crosslinking or breaking of polymer chains co-occurs, affecting the material's physical, chemical, and surface properties [14,24–26]. Determining the effect of gamma irradiation on the properties of electro-spun PCL scaffolds is one of the objectives of this paper. There has been little research performed to understand the effects of sterilization, especially gamma irradiation, on the structural modification of PCL scaffolds [13,14,22–24,26]. In a study by Dominik de Cassan et al. the sterilization of PCL by gamma radiation led to polymer chain scission and reduced the average molecular weight ($\overline{M}_n$) [22]. Augustine et al. studied the dose-dependency of gamma radiation on the material properties of electro-spun PCL tissue engineering scaffolds. The presence of OH (hydroxyl) and COOH- (carboxyl) functional groups in the PCL membrane after irradiation and no significant change in the tensile properties was uncovered by the researchers [13].

No study has been done on multi-variate, multi-objective optimization of the production of PCL skin scaffold by RSM. This study aims to study multi-variate, multi-objective optimization of the production conditions for the PCL skin scaffold using RSM to find the optimal conditions based on four critical electrospinning factors (polymer concentration (wt%), applied voltage (kV), nozzle-collector distance (cm), and flow rate (ml/h)) and three different mechanical responses (Young's modulus, elongation-at-break and, tensile strength). After obtaining appropriate models from RSM, the effects of electro-spun process variables on the related responses were investigated using Sobol's sensitivity analysis. After that, the optimal PCL skin scaffold was sterilized by different gamma-ray doses of

25, 40, and 55 kGy to check how the gamma-ray sterilization can affect the PCL physical and mechanical properties of PCL characterization analyses, including tensile test, XRD, FTIR, and SEM analysis was performed to evaluate the performance of the scaffolds.

2. Materials and methods

Polymer solutions for electrospinning were prepared using only polycaprolactone (PCL, Mw = 80,000), chloroform ($CHCl_3$, 99.8 % purity), and an Acetone mixture. The PCL and all solvents were acquired from Merck (Germany).

2.1. Preparation of PCL fibers by electrospinning

Solutions were made of PCL with concentrations of 10, 11, and 12 % (w/v), dissolved in chloroform and acetone with a 1:1 solvent mass ratio. The solutions were stirred (200 rpm) for 1 h to substantiate the complete dissolving. Electrospinning with Nano Fiber Electrospinning Unit -Full Option Lab2 ESI-II model was performed under room conditions. Fig. 1 shows the Electrospun nanofibrous fibers. The average of PCL thicknesses was about 0.08 mm with smooth surfaces.

2.2. Multi-variate, multi-objective experimental design

The statistical software package Design-Expert11, Response surface methodology (RSM) was used for regression analysis of the experimental data [15,16,27]. The goal in such designs is to optimize the responses which are affected by several independent variables. In each experiment, changes in the input variables are made to determine the impacts of the changes on the response variable. Using the multi-variate, multi-objective optimization RSM method, the effects of four major independent variables of polymer concentration (wt%), applied voltage (kV), nozzle-collector distance (cm), and flow rate (ml/h) on the electrospinning process, were evaluated. The response objective functions were selected as a Young's modulus, elongation-at-break, and tensile strength. The Box-Behnken design with five central points was selected with 29 designed experiments to determine the relationship between 4 parameters and 3 responses. for four variables with three levels of change, a Box-Behnken design and its purposes were suitable experimental designs. The responses were used to develop an empirical model that correlated the responses to the four major independent variables in the electrospinning process using reduced linear, reduced 2FI, and reduced quadratic models. The general form of a second-degree polynomial equation is given by Eq. (1). One could get a linear equation by removing the interaction and quadratic coefficients and a 2FL equation by removing the quadratic coefficients of Eq. (1).

$$Y = \acute{b}_0 + \sum_{i=1}^{n} b_i X_i + \sum_{i=1}^{n} b_{ii} X_i^2 + \sum_{i=1}^{n} \sum_{j>1}^{n} b_{ij} X_i X_j \tag{1}$$

where Y, b, and X stands for the predicted response, coefficient, and independent variable, respectively, $\acute{b}_0$ is the constant coefficient, b_i is the linear coefficient, b_{ij} is the interaction coefficients, b_{ii} is the quadratic coefficients, and x_i, x_j are the coded values of variables [15].

The lack of fit measures the quality of the fit between the data and the selected model. If the expression's lack of fit is significant, the polynomial model does not correctly fit the plotted points. To estimate the statistical significance of the variables, the analysis of variance (ANOVA) was used. The fit quality was evaluated by R2 and predicted R2 (Pred-R2) functions. R2 values indicate whether the obtained models could correlate well with the experimental values. Pred-R2 is a suitable measure to evaluate the performance of the predictive power of the offered mode [27]. significance of the model's parameters was provided by p-value examination. This analysis implies that if the P-values are less than 0.05 indicate that the model terms are significant. Response levels to distinguish the unique and interactive effects of the variables on the responses are shown in Table 1.

Fig. 1. Electrospun nanofibrous fibers made in the laboratory.

Table 1
Experimental range of independent process variables.

Level (actual)				
Parameter	**Units**	**Lower**	**Center**	**Upper**
Concertation(X1)	wt.%	10	11	12
Distance from needle(X2)	cm	10	12.5	15
Flow rate(X3)	ml/h	1	2	3
Voltage(X4)	kV	18	20	22

2.3. Sobol's sensitivity analysis

Variance-based sensitivity analysis (Sobol method) is a form of global sensitivity analysis [28,29]. Working within a probabilistic framework, it decomposes the variance of the output of the model or system into fractions that can be attributed to inputs or sets of inputs. This method estimates the significance of the input parameters of a mathematical model by providing a "global sensitivity index" to a parameter's unique and interactive impacts. Then, a "total sensitivity index" is computed from the global indices that reflect an independent factor predicting the total effect of the variations of the variables on the objective function [30].

2.4. Exposure to gamma irradiation

Electro-spun PCL scaffolds were irradiated with ^{60}Co γ-source. It has two gammas with 1.17 and 1.33 MeV energy at a dose rate of 4.2 kGy/h with an accumulated dose of 25, 40, and 55 kGy. ^{60}Co gamma irradiation experiment (cylindrical irradiation chamber with a length of 19 cm and diameter of 14 cm) was conducted at the Atomic Energy Organization of Iran.

2.5. Characterization tests

2.5.1. Mechanical characterization

The effect of gamma irradiation on the mechanical properties of the PCL scaffolds has been evaluated using tensile testing. Gamma irradiated and unirradiated samples were cut into rectangles, 30 mm in length and 5 mm in width, and were designed to place into the mechanical testing machine leaving a 1 cm gauge length for mechanical loading. A tensile strength test was conducted on the scaffold by a Santam STM-50 bench test machine. The average values of the mechanical properties were obtained from the results of three tests. Samples were stretched until rupture.

2.5.2. X-ray diffraction (XRD)

The XRD analysis was performed to understand the change in the crystallinity of the electro-spun PCL nanofibers after the gamma irradiation. The analysis was performed in a diffractometer (PHILIPS model X'pert – PW3040/60, with Cu anode and wavelength 1.54A°).

2.5.3. Scanning electron microscopy (SEM)

The morphological properties of the PCL scaffolds before and after gamma irradiation were determined by scanning electron microscopic (SEM) analysis. A TESCAN VEGA SEM was used to analyze the samples.

2.5.4. Fourier transform infrared spectroscopy

Fourier transform infrared (FTIR) analysis has been carried out on the PCL scaffolds before and after the gamma irradiation to understand the changes in the surface functional groups caused by the irradiation. FTIR spectra were obtained using a Bruker ALPHA FTIR Spectrometer.

Table 2
Summary of the range of mechanical properties of various electro-spun PCL scaffolds.

Young's modulus (MPa)	Fiber diameter (μm)	Elongation at break (%)	Tensile strength (MPa)	
15–104	0.261 ± 0.004	73.12–137.27	2.52–30.07	This study
10–160	–	–	1–9	[18]
10–80	0.9–8	5–20	4.34–13.17	[31]
19–55	1.01–3.37	6.2–62.5	4–13	[33]
53 ± 36	0.44–1.04	98 ± 30	12 ± 7	[32]
15–127	0.903–3.661	–	–	[17]
–	0.305–3.25	–	0.5–3	[15]

Table 3
RSM experimental design matrix and results.

Run	Factor 1	Factor 2	Factor 3	Factor 4	Experimental results	Predicted values	Experimental results	Predicted values	Experimental results	Predicted values
	A Concertation	**B Distance from needle**	**C Flow rate**	**D Voltage**	**Young's modulus (Response 1)**	**Young's modulus (Response 1)**	**Elongation at break (Response 2)**	**Elongation at break (Response 2)**	**Tensile strength (Response 3)**	**Tensile strength (Response 3)**
	wt.%	**cm**	**ml/h**	**V**	**MPa**	**MPa**	**%**	**%**	**MPa**	**MPa**
1	10	12.5	3	20	90.00	84.75	90.95	93.39	30.07	26.74
2	11	12.5	3	18	124.00	–	115.71	109.48	37.11	–
3	11	12.5	2	20	35.00	36.17	112.31	103.67	24.45	17.40
4	11	12.5	3	22	49.00	51.97	120.97	120.81	20.82	20.23
5	12	12.5	2	18	73.00	64.92	117.45	119.76	24.41	23.02
6	12	12.5	3	20	45.00	47.47	137.27	136.90	13.01	11.52
7	12	10	2	20	59.00	55.37	136.40	125.43	25.63	24.41
8	12	12.5	1	20	104.00	106.35	117.03	113.95	30.02	30.36
9	11	15	1	20	21.32	23.97	94.25	92.20	13.04	12.21
10	11	12.5	2	20	38.00	36.17	93.73	103.67	16.18	17.40
11	12	12.5	2	22	70.50	64.63	133.32	131.09	21.32	18.85
12	10	15	2	20	15.00	15.04	74.84	81.92	8.07	10.40
13	11	12.5	2	20	40.67	36.17	76.96	–	17.50	17.40
14	11	10	3	20	35.50	42.71	94.93	–	17.15	22.60
15	10	10	2	20	30.00	26.15	89.69	81.92	18.44	17.34
16	10	12.5	2	22	35.00	35.41	96.87	87.58	18.40	18.16
17	11	10	1	20	35.32	35.08	101.86	92.20	19.92	19.15
18	11	12.5	1	18	42.00	44.64	73.12	86.54	13.56	14.58
19	11	15	2	18	22.00	15.80	107.50	98.01	15.00	12.83
20	11	12.5	1	22	46.32	44.34	88.55	97.86	16.65	16.78
21	11	15	3	20	39.00	31.60	109.55	115.15	17.33	15.65
22	11	10	2	18	31.00	26.91	93.55	98.01	20.88	19.78
23	11	12.5	2	20	31.50	36.17	99.01	103.67	11.07	17.40
24	12	15	2	20	31.50	44.26	123.15	125.43	14.23	17.46
25	11	12.5	2	20	34.00	36.17	99.57	103.67	11.62	17.40
26	10	12.5	2	18	21.67	35.70	74.17	76.26	8.74	9.58
27	11	10	2	22	22.00	26.64	98.22	109.33	9.15	–
28	10	12.5	1	20	16.00	10.62	77.08	70.45	2.52	1.00
29	11	15	2	22	17.32	15.51	111.51	109.33	14.65	15.03

3. Results and discussion

3.1. Development of regression model equation

Electro-spun PCL nanofibers, which mimic the extracellular matrix, have been produced with various solvents and combinations. The Box-Behnken design was used to develop a correlation between the four electrospinning effective variables to the mechanical properties of the PCL scaffold. The quadratic model for Young's modulus, the 2FL model for the tensile strength, and the linear model for the elongation-at-break were selected as suggested by the software. To obtain the most accurate models, the experimental results that were not in the ranges of the statistical charts of the models were removed. Mechanical values for Young's modulus, fiber diameter, elongation-at-break, and tensile strength of PCL scaffolds obtained in similar studies are given in Table 2, to be compared with the ranges obtained in our work. The nanofibrous scaffolds detailed in various studies are predominantly produced using the electrospinning method [15,17,31,32], Repana et al. specifically employed the coaxial electrospinning technique. This method, a modification of electrospinning, produces core-shell structures that offer advantages such as delayed diffusion and protection of delicate biomolecules [33].

The design of the experiments is shown in Table 3, together with the experimental and RSM-predicted values for the responses. The analysis of variance (ANOVA) results is shown in Table 4. The F-values imply that the models are significant. There is only a 0.01 % chance that an F-values could occur due to noise. P-values (a measure of statistical significance) show that the obtained models are significant and can properly be used to predict the related mechanical properties of the PCL scaffold. Table 4. Part (a) shows the Lack of Fit. An f-value of 4.03 implies that there is a 9.36 % chance that such a Lack of Fit F-value could occur due to noise. This relatively low probability (<10 %) is troubling. In Table 4 parts (b) and (c) the Lack of Fit F-value are 0.88 and 0.20, respectively. It implies that the Lack of Fit is insignificant relative to the pure error. R^2 for the Young's modulus, elongation-at-break, and tensile strength models were 0.9350, 0.8542, and 0.8044, respectively. The Predicted R^2 of 0.8442, 0.8009, and 0.6995 are in reasonable agreement with the

Table 4
The analysis of variance of the response surface different models for a) Young's modulus, b) elongation at break, and c) tensile strength.

a) Response 1: Young's modulus

Source	Sum of Squares	Degree of freedom	Mean Square	F-value	p-value	
Reduced Quadratic Model	11808.09	8	1476.01	34.18	<0.0001	significant
X1-Concentration	2561.81	1	2561.81	59.32	<0.0001	
X2-Distance from needle	370.37	1	370.37	8.58	0.0086	
X3-Flow Rate	156.24	1	156.24	3.62	0.0724	
X4-Voltage	0.2322	1	0.2322	0.0054	0.9423	
X1X3	4422.25	1	4422.25	102.40	<0.0001	
X1X1	1277.66	1	1277.66	29.59	<0.0001	
X2X2	1460.82	1	1460.82	33.83	<0.0001	
X3X3	949.13	1	949.13	21.98	0.0002	
Residual	820.51	19	43.18	–	–	
Lack of Fit	769.62	15	51.31	4.03	0.0936	not significant
Pure Error	50.89	4	12.72	-		
Cor Total	12628.60	27	–	–		

b) Response 2: Elongation-at-break

Source	Sum of Squares	Degree of freedom	Mean Square	F-value	p-value	
Reduced Linear Model	7506.36	3	2502.12	44.91	<0.0001	significant
X1-Concentration	5678.42	1	5678.42	101.92	<0.0001	
X3-Flow rate	1443.14	1	1443.14	25.90	<0.0001	
X4-Voltage	384.80	1	384.80	6.91	0.0150	
Residual	1281.37	23	55.71	–	–	
Lack of Fit	1094.71	20	54.74	0.8797	0.6418	not significant
Pure Error	186.66	3	62.22	–	–	
Cor Total	8787.73	26	–	–	–	

c) Response 3: Tensile strength

Source	Sum of Squares	Degree of freedom	Mean Square	F-value	p-value	
Reduced 2FI Model	859.80	6	143.30	13.71	<0.0001	significant
X1-Concentration	149.77	1	149.77	14.32	0.0012	
X2-Distance from needle	131.05	1	131.05	12.53	0.0021	
X3-Flow Rate	32.30	1	32.30	3.09	0.0941	
X4-Voltage	11.92	1	11.92	1.14	0.2984	
X1X3	496.70	1	496.70	47.50	<0.0001	
X1X4	40.64	1	40.64	3.89	0.0627	
Residual	209.11	20	10.46	–	–	
Lack of Fit	92.00	16	5.75	0.1964	0.9923	not significant
Pure Error	117.12	4	29.28	–	–	
Cor Total	1068.92	26	–	–	–	

Adjusted R^2 of 0.9077, 0.8352, and 0.7457 for the Young's modulus, elongation-at-break, and tensile strength, respectively, i.e., the difference is less than 0.2.

Regression analysis was performed to fit the response functions of Young's modulus, elongation at break, and tensile strength. In the models, variables take their coded values, represent Young's modulus (Y1), elongation at break (Y2), and tensile strength (Y3) as functions of process parameters as a polymer concentration (X1), nozzle-collector distance (X2), flow rate (X3), and applied voltage (X4) [3]. The final empirical models in terms of the coded factors after removing the insignificant terms are shown in Table 5. The coded equation is useful for identifying the relative impact of the factors by comparing the factor coefficients. A positive sign in front of the terms shows a synergistic effect of variables, whereas a negative sign shows an adversary effect.

3.2. Statistical analysis

Important information on the effects of the variables on the responses can be derived from the 3-dimensional binary interaction plots. The interactions between the variables can also be understood by the contour plots at the bottom of each graph. More effective variables on the responses are in tune with sharper curvature in the curves. Figs. 1–3 show the three-dimensional response surfaces, the combined effects of concentration, voltage, nozzle-collector distance, and flow rate on the Young's modulus, elongation-at-break and tensile strength responses, respectively. Polymer scaffolds are used for skin repair; where the Young's modulus must be in the optimal range of 4.5–20 MPa [19]. From Fig. 2(a), it can be inferred that the applied voltage has no effect, and only lower polymer concentrations affect Young's modulus and keep us closer to the optimal conditions. In Fig. 2(b), lower casting solution concentration as well as greater nozzle-collector distance, and in plot (c), the lower polymer concentration and flow rate provide better conditions for obtaining Young's modulus in the acceptable range. As seen in Fig. 2(c), the polymer concentration and flow rate cause more curvature in the response surface of the Young's modulus, which shows that the interaction between these two variables is more effective than those of the other variables. Concentration and flow rate positively correlated the Young's modulus, while nozzle-collector distance and applied voltage showed an opposite trend. This means that higher-level settings of concentration and flow rate will result in scaffolds with higher elastic modulus, as mentioned in other similar research [17].

The optimal range of elongation-at-break for skin scaffold is between 70 and 77 % [21]. As seen in Fig. 3(a), lower values of applied voltage and concentration bring us closer to the optimal range. Also, Fig. 3(b) shows the insignificance of the nozzle-collector distance term, which was removed earlier in the experimental equations. An optimal response range could be reached at low polymer concentration and flow rate in Fig. 3 (c).

Regarding the tensile strength response, considering the optimal range for the scaffolds applications in wound healing, which is between 2 and 16 MPa, it can be seen in Fig. 4(a) that the applied voltage is not significant. At the same time, the lower value of polymer concentration will be appropriate for this purpose. As it was mentioned in the study of Asvar et al. it was observed that at a constant value of applied voltage, an increase in the polymer concentration increased the tensile strength [15].

It can be seen in Fig. 4(b) that the nozzle-collector distance was not a significant affecting variable on the tensile strength response. This is also mentioned in the study of Asvar et al. [15]. Fig. 4(c) shows two suitable areas for the desired tensile strength range for the skin scaffold; low values of polymer concentration and flow rate as well as high values of polymer concentration and flow rate can be suitable to achieve the desired tensile strength values.

3.3. Process optimization

In the production of PCL scaffolds, one of the main aims of this study was to find the optimal electrospinning process conditions for obtaining scaffolds with desired mechanical characteristics, which are in the normal ranges observed for human skin healing. Therefore, the PCL scaffolds must possess appropriate mechanical properties to accommodate different types of skin wounds. The desirability function was applied using Design-Expert software version 11 to optimize these responses under the considered mechanical conditions and compromise them. The experimental conditions with the highest desirability were chosen to confirm the equations and continue the studies of this research. The optimal mechanical properties of the PCL skin scaffold were obtained as the conditions obtained in run 12 (Table 3), as shown in Fig. 5. The PCL scaffold was prepared under the optimal experimental conditions given in Table 6. It was observed that the experimental values were in good agreement with the models-predicted values.

3.4. Sobol's sensitivity results

Sobol's sensitivity analysis for (a) Young's modulus, (b) elongation-at-break, and (c) tensile strength concerning four main independent variables in the electrospinning process was performed by calculating the Sobol's total order indices for the experimental models presented with the determined equations. The results of this investigation are presented in Fig. 6(a) shows that flow rate is the

Table 5
Final equation in terms of coded factors.

Response	Intercept	X1	X2	X3	X4	X1X3	X1X4	X1X1	X2X2	X3X3
Y1	36.1719	14.61	−5.56	3.81	−0.146	−33.25	–	13.99	−14.96	12.13
Y2	103.672	21.75	–	11.47	5.66	–	–	–	–	–
Y3	17.4037	3.53	−3.47	1.72	1.101	−11.14	−3.19	–	–	–

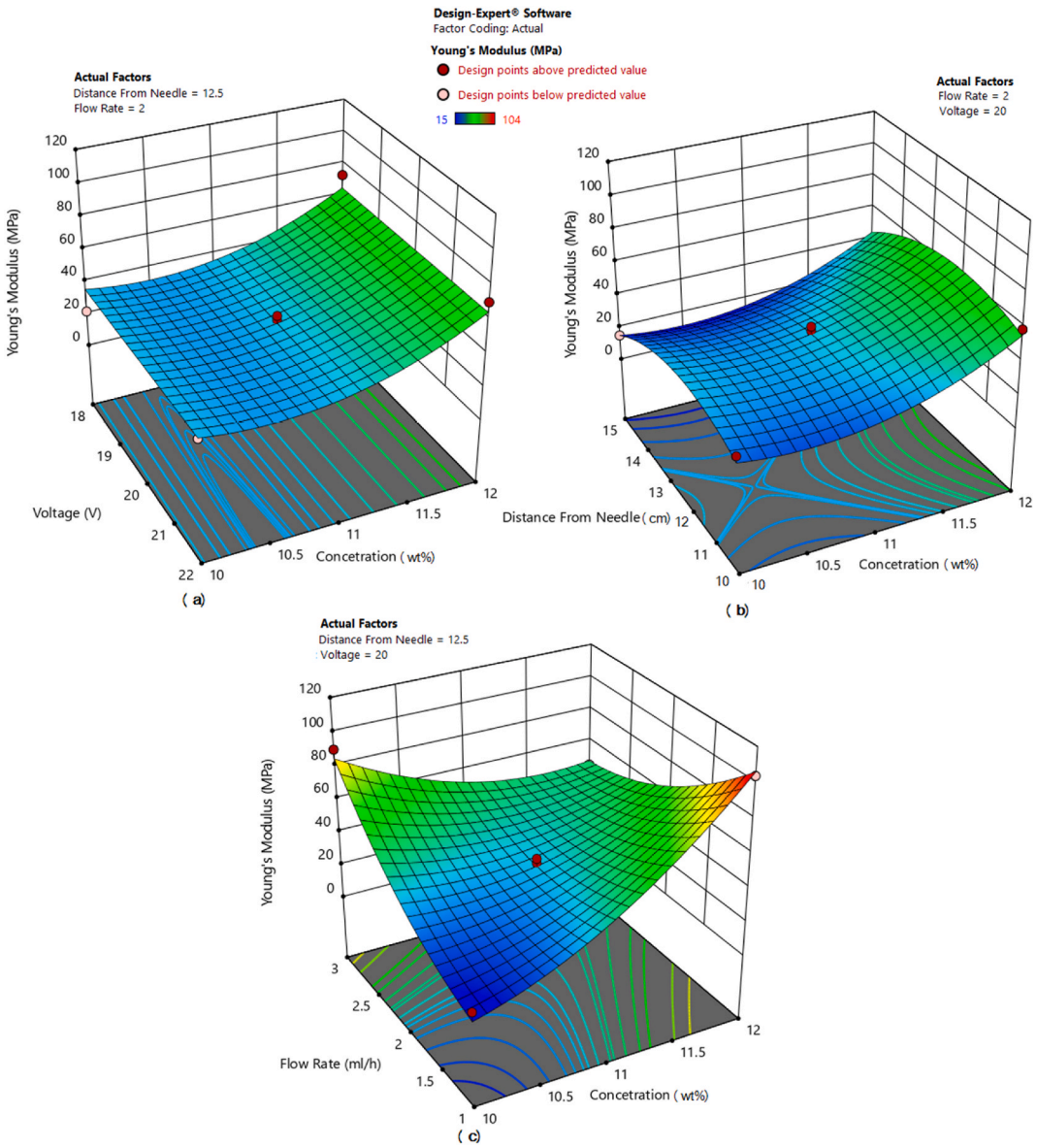

Fig. 2. Three-dimensional response surfaces, the combined effect of concentration, voltage, nozzle-collector distance, and flow rate for Young's modulus response.

most influential parameter on the Young's modulus response (76.45 %). The following order is the polymer concentration (14.28 %). The interaction of these two parameters causes a significant curvature in the response of Young's modulus, which shows the importance of a correct selection to reach the appropriate range of the desired response. As mentioned earlier, the applied voltage does not affect Young's modulus response. In Fig. 6(b), the polymer concentration is a more effective parameter (64.35 %) on the elongation-at-break compared to the two variables of flow rate (17.64 %) and voltage (18.01 %). The nozzle-collector distance parameter does not affect this response. Fig. 6(c) shows that the polymer concentration (39.48 %) and flow rate (41.27 %) are the most critical parameter in tensile strength responses, and voltage (15.39 %) is the next most important. The nozzle-collector distance parameter is insignificant for the tensile strength response.

3.5. Characterizations

3.5.1. FTIR analysis

The impact of gamma radiation on the functional groups of the PCL scaffold was determined by FTIR analysis. The FTIR spectrum of the PCL scaffold before and after irradiation with different gamma radiation doses is shown in Fig. 7. The FTIR spectrum before

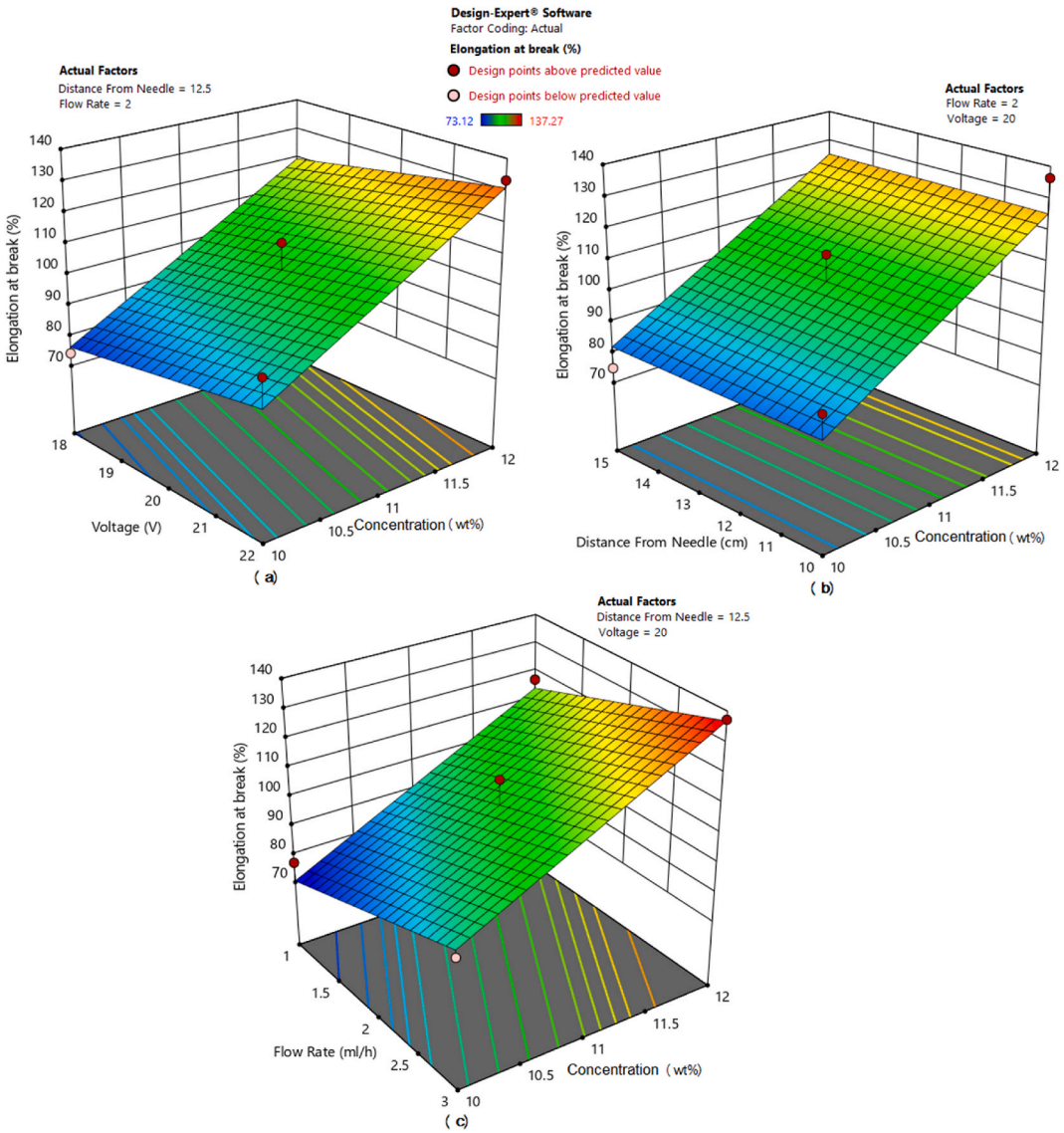

Fig. 3. Three-dimensional response surfaces, the combined effect of concentration, voltage, nozzle-collector distance, and flow rate for elongation at break response.

irradiation shows a peak at 1720 cm^{-1} due to the carbonyl ester group, which corresponds to the –CO group in PCL. The peak at 2854 cm^{-1} corresponds to stretching vibration of C–H bound related to aliphatic carbons [13,34]. Apart from these characteristic peaks, additional peaks were observed in the range of 3529 and 3441 cm^{-1} in the gamma-irradiated scaffold related to the tensile vibrations. These peaks indicate the presence of the OH (hydroxyl) functional group in the PCL scaffold after irradiation due to the breakup of the ester bonds [13]. Polyesters such as PCL have ester bonds on their leading chains that are susceptible to breakage. It was said that gamma radiation causes the cutting of polymer molecular chains and breaks them into smaller pieces [13]. FTIR analysis showed that gamma radiation could affect the polymer chain because of the presence of the O–H stretching band. Some absorbances between 2000 and 2500 cm^{-1} in the FTIR spectrum are related to forming CO_2 band after gamma irradiation. The overall results suggest that the gamma irradiation had a significant effect on increasing the volatile compounds such as CO_2 detected in the Polycaprolactane specimens and the formed band is related to the CO_2 that was formed at these irradiation dosages [35].

Gamma radiation can damage the polymer molecular structure due to direct energy transfer to molecules or secondary electrons released by ionization. In addition, high-energy gamma radiation leads to the generation of free radicals (that will increase the density of the presence of triple bonds in the chain), scission of the leading chains, or cross-linking that subsequently changes the size distribution of the chains in the bulk polymer [13].

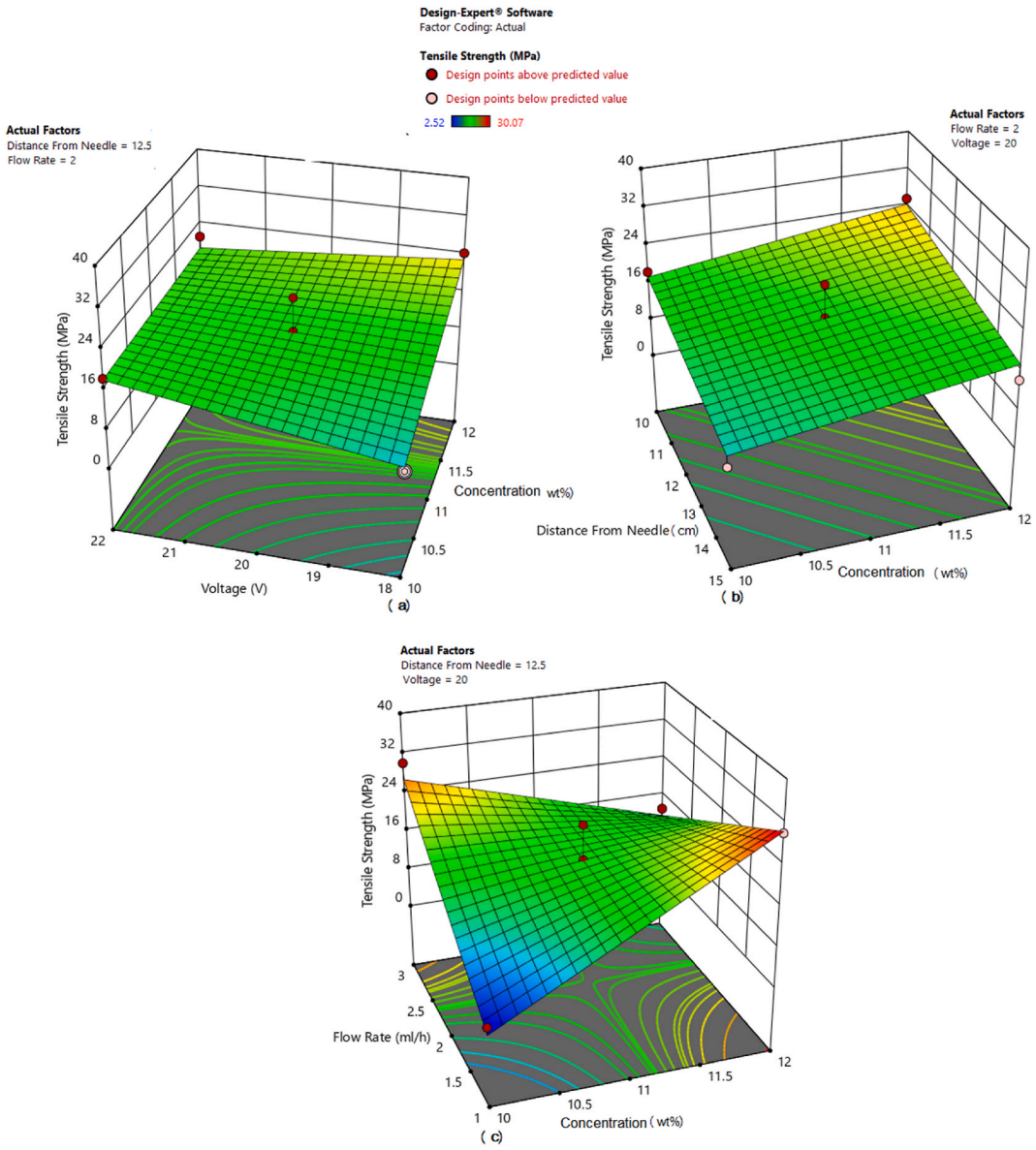

Fig. 4. Three-dimensional response surfaces, the combined effect of concentration, voltage, nozzle-collector distance, and flow rate for tensile strength response.

3.5.2. XRD analysis

Because crystallinity affects the material's mechanical properties, how the polymer's crystallization changes during the gamma radiation process is important. Fig. 8 shows the XRD spectrum of the optimal non-irradiated and irradiated scaffolds. PCL is a semi-crystalline polymer and contains both crystalline and amorphous regions. The results show that the electro-spun PCL scaffold contains three distinct reflections at Bragg angles of about 21.4, 22.0, and 23.7, which correspond to the (110), (111), and (200) planes of the orthogonal crystal structure, respectively [36]. To obtain quantitative information about the changes in the crystallinity percentage of PCL scaffolds due to gamma radiation, the ratio of the area under the curve of the diffraction peaks and the amorphous void area were calculated and shown in Table 7. The crystallinity percentage of the non-irradiated PCL scaffolds was 32.47 %. The highest percentage of crystallinity among the studied samples was 36.56 %, obtained for the sample irradiated with 55 kGy. The results show that exposure to higher gamma doses leads to an increase in the intensity of the diffraction peaks reflecting an increase in the crystallinity, which causes a more regular arrangement of the crystals [13]. This tendency can be seen in radiation doses of 40 and 55 kGy. The decrease in the amorphous nature of the polymer and the increase in crystallinity with increasing dosage may be due to the scission of the polymer chains, as a result of which the polymer undergoes spatial rearrangement, and the tiny fragments may rearrange themselves towards a new crystalline region [37]. While in the case of the sample irradiated with 25 kGy, there was a slight decrease in

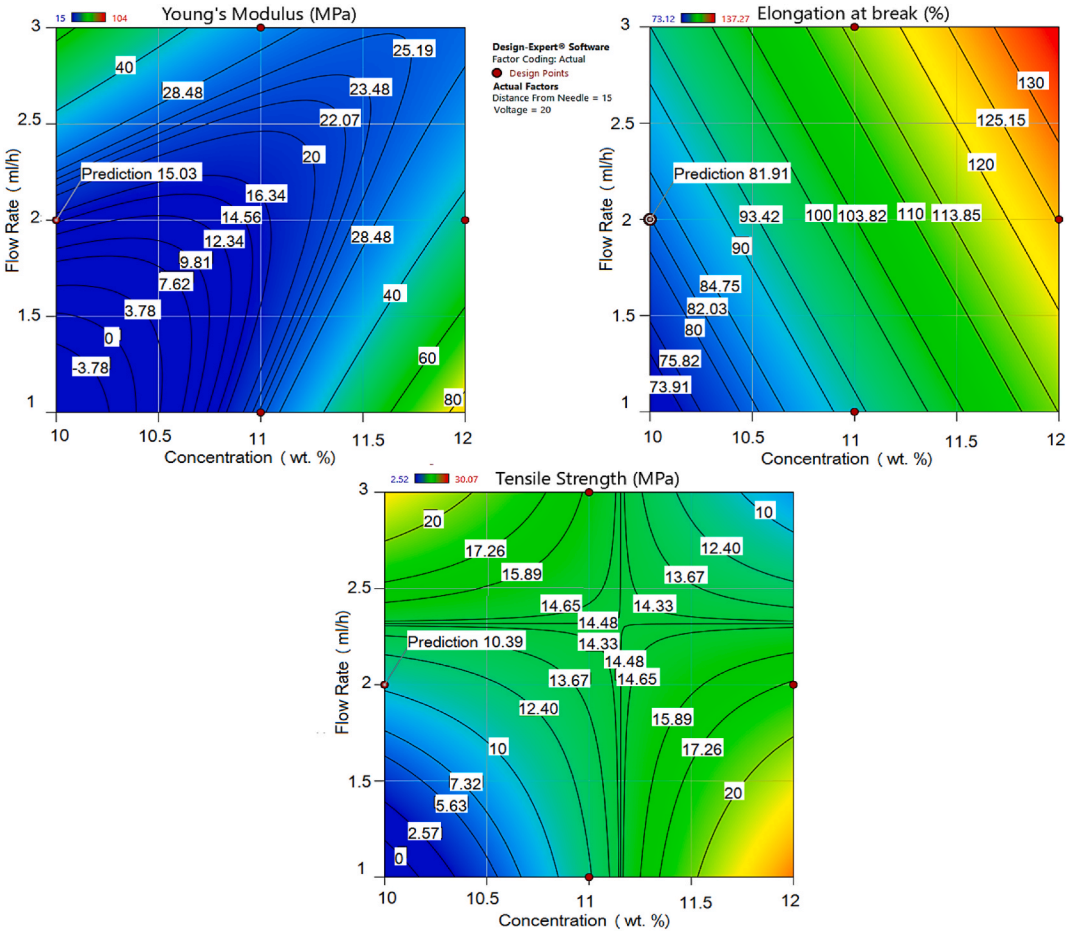

Fig. 5. The optimum region on the polymer concentration and flow rate for the production of skin scaffold by mechanical responses: (a) Young's modulus, (b) elongation at break, and (c) t ensile strength, respectively.

Table 6
Model validation.

Concentration	Nozzle-collector distance	Flow rate	Voltage	Young's modulus		Elongation-at-break		Tensile strength	
				Predicted	Experimental	Predicted	Experimental	Predicted	Experimental
10	15	2	20	15.036	15.9	81.92	74.85	10.39	8.07

the intensity compared to the non-irradiated sample, and the crystallinity percentage decreased. A lower irradiation dose decreases crystallinity due to the dominance of cross-linking over the breaking of the chains, which turns ordered crystals into disordered ones by creating new bonds between neighboring chains [13].

3.5.3. Morphology

SEM analysis was employed to investigate the effect of gamma radiation on the morphology and microstructure of electro-spun PCL scaffolds. It is obvious from the scanning electron micrographs of PCL scaffolds (Fig. 9) that the mean fiber diameter (equal to 0.272 ± 0.02 μm) remained unchanged. It is also clear that there is no significant change in the fibrous morphology as a result of the gamma irradiation. In addition, there were no apparent signs of damage across the applied irradiation dose range in the scaffolds.

3.5.4. Mechanical test

From the tensile measurements, it can be seen in Table 8 and Fig. 10 that the tensile strength and Young's modulus increased with the increase of gamma radiation dose, which is in agreement with those obtained by Augustin et al. [13]. Irradiation can change the molecular structures of the polymer by either chain scission, which reduces tensile strength and elongation, or crosslinking, which increases tensile strength but reduces elongation [24,38,39]. This change in elongation-at-break and tensile strength can be explained

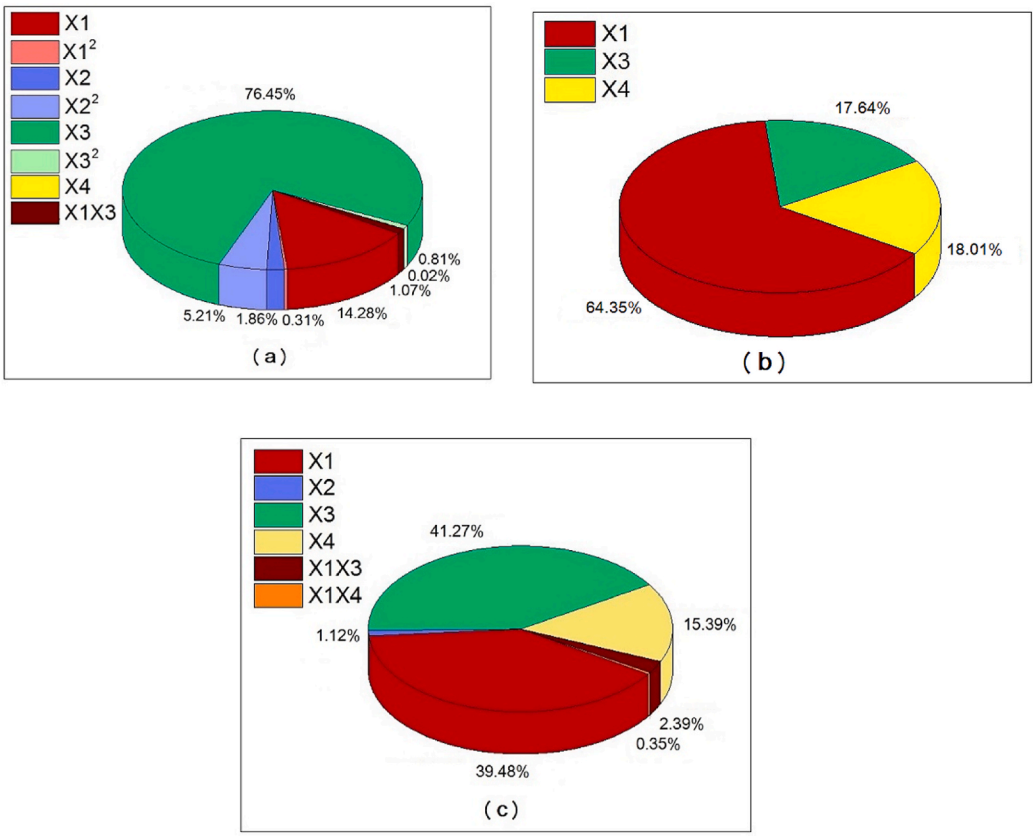

X1: Polymer concentration, X2: Nozzle-collector distance, X3: Flow rate, and X4: Applied voltage.

Fig. 6. Sobol's sensitivity results of (a) Young's modulus, (b) elongation at break, and (c) tensile strength to four major independent variables in the electrospinning process.

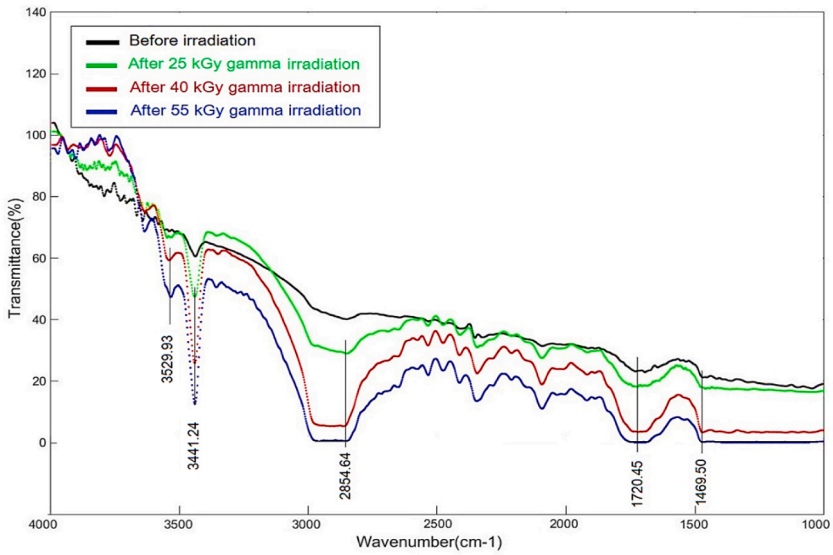

Fig. 7. FTIR spectrum of electro-spun PCL scaffold after exposure to different doses of gamma radiation.

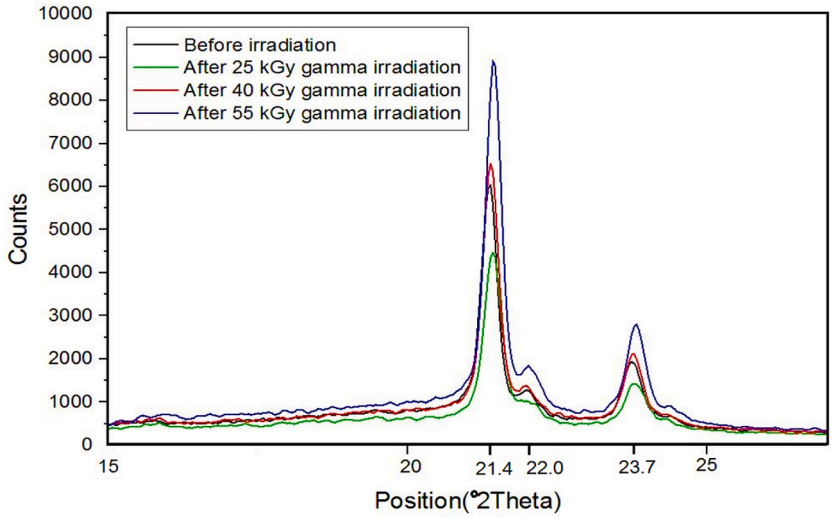

Fig. 8. XRD spectrum of optimal electro-spun PCL scaffold irradiated with different doses of gamma radiation.

Table 7
Change in crystallinity percentage of PCL scaffold due to gamma radiation.

Irradiated Dose (kGy)	Crystallinity (%)
0	32.47
25	31.46
40	33.52
55	36.56

in terms of polymer chain scission and crosslinking. It is expected that in 40 kGy and 55 kGy radiation doses, the crosslinking has overcome the breaking of the chains because Young's modulus has increased significantly, and the elongation-at-break has decreased. Since the crosslinks between polymer chains are stronger than conventional intermolecular attractions, crosslinking forms a more stable and stronger polymer network but generally leads to a decrease in impact strength, and the polymer becomes brittle with increasing the gamma irradiation dosage [24]. Cross-linking can create three-dimensional networks in the scaffold structure that can improve the properties of the polymer. At the same time, the crystallinity factor and, thus, density may also change as chain scission continues [24,40]. For a radiation dose of 25 kGy, the mechanical properties of Young's modulus and mechanical strength have increased. Considering that elongation-at-break has also increased in this dose, it can be concluded that radiation has modified the structure of this sample and improved its mechanical properties. It is important because soft tissues like skin experience large strains, and the scaffolds must adapt and still elastically [31]. The XRD test results also confirmed the improvement of the polymer structure because crystallinity decreased in 25 kGy doses compared to the non-irradiated sample. The increase in amorphousness of the structure is synonymous with the increase in crosslinking, which did not cause the loss of elongation at break. The irradiated sample under the dose of 25 kGy is a sample with improved mechanical properties after sterilization and provides suitable mechanical properties for use as a skin scaffold.

4. Conclusions

This study revealed electrospinning factors that significantly affect the production of an ideal electro-spun PCL scaffold with desired mechanical properties for skin wound dressing by applying the RSM methodology and multi-variable, multi-objective optimization techniques. For Young's modulus and tensile strength, the flow rate was the most significant factor with 76.45 %, and 41.27 % impact shares, respectively. The polymer concentration is the following significant parameter on elongation at break, tensile strength and, Young's modulus responses with 64.35 %, 39.485 and, 14.28 % impact share, respectively. However, the nuzzle-collector distance has an inferior impact. A regression model was developed describing the quantitative relationship between the significant factors and corresponding responses. Using these models, optimal conditions could be estimated to obtain a PCL skin scaffold with ideal mechanical properties. Sobol's total order indices for the experimental models were also calculated. Based on RSM results and the production of optimized PCL skin with desired mechanical properties (under solution concentration of 10 % w/v, the flow rate of 2 mL/h, nuzzle-collector distance of 15 cm, and applied voltage 20 kV), for clinical operations they must be sterilized. Therefore, the sterilizability of the PCL scaffold with gamma irradiation and its effect on the material's properties have been investigated. The SEM analysis showed no significant change in fibrous morphology as a result of gamma irradiation at any dosage. The FTIR analysis showed

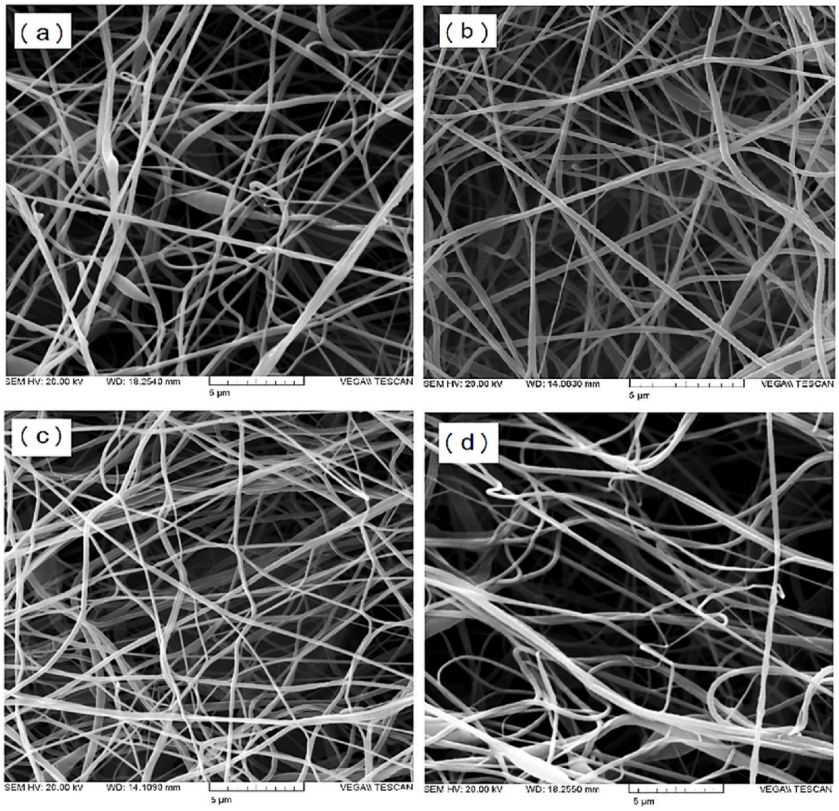

Fig. 9. SEM images of the optimal PCL electrospinning sample (a): before and after gamma irradiation with (b): 25, (c): 40 and, (d): 55 kGy doses.

Table 8
Change of optimal tensile properties of electro-spun PCL scaffold caused by gamma radiation.

Irradiated dose(kGy)	Young's modulus (MPa)	Elongation-at-break (%)	Tensile strength (MPa)
0	15 ± 2	74.84 ± 5	8.07 ± 1
25	15.9 ± 2	107.79 ± 16	9.57 ± 1
40	22.6 ± 3	62.55 ± 8	10.63 ± 2
55	19.05 ± 2	50.31 ± 1	8.41 ± 1

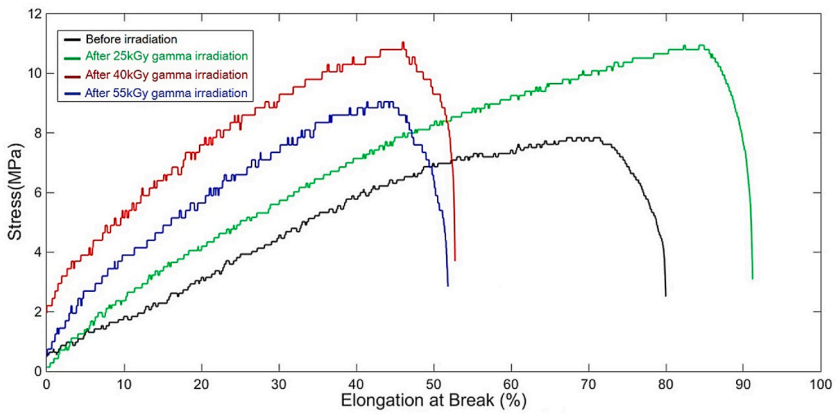

Fig. 10. Stress-strain curve for optimal PCL electro-spun scaffold after irradiation with different doses of gamma rays.

the presence of –OH (hydroxyl) functional groups in the PCL scaffold after the irradiation due to the breakup of ester bonds. The XRD results show that exposure to a higher gamma dose leads to an increase in crystallinity. While in the case of the sample irradiated with 25 kGy, the crystallinity decreased compared to the not irradiated sample (31.46 % and 32.47 % respectively). Tensile property for a radiation dose of 25 kGy showed that Young's modulus and mechanical strength have increased. Considering that elongation-at-break has also increased in this dose, it can be concluded that radiation has modified the structure of the optimal PCL scaffold and improved its mechanical properties. Hence, 25 kGy is an optimum radiation dose, and this sample has the necessary features for use as a skin scaffold.

Ethical approval

This article does not contain any studies with human participants or animals performed by any of the authors.

Data availability statement

The data associated with the study has not been deposited into a publicly available repository.

CRediT authorship contribution statement

M. Hoseini: Writing – review & editing, Writing – original draft, Visualization, Validation, Software, Resources, Project administration, Methodology, Investigation, Funding acquisition, Formal analysis, Data curation. **S. Hamidi:** Writing – review & editing, Supervision, Project administration, Funding acquisition. **E. Salehi:** Writing – review & editing, Methodology, Data curation, Conceptualization. **A. Mohammadi:** Validation, Supervision, Resources, Project administration. **F. Mirhoseini:** Investigation, Data curation, Conceptualization. **M. Ravaghi:** Methodology, Data curation.

Declaration of competing interest

Mahsa Hoseini reports were provided by Arak University. If there are other authors, they declare that they have no known competing financial interests or personal relationships that could have appeared to influence the work reported in this paper.

References

[1] G.Z. Tan, Y. Zhou, Electrospinning of biomimetic fibrous scaffolds for tissue engineering: a review, Int. J. Polym. Mater. Polymeric Biomater. 69 (15) (2020) 947–960.
[2] M. Janmohammadi, M. Nourbakhsh, Electrospun polycaprolactone scaffolds for tissue engineering: a review, Int. J. Polym. Mater. Polymeric Biomater. 68 (9) (2019) 527–539.
[3] O. Suwantong, Biomedical applications of electrospun polycaprolactone fiber mats, Polym. Adv. Technol. 27 (10) (2016) 1264–1273.
[4] G.H. Kim, Electrospun PCL nanofibers with anisotropic mechanical properties as a biomedical scaffold, Biomed. Mater. 3 (2) (2008) 025010.
[5] A. Cipitria, et al., Design, fabrication and characterization of PCL electrospun scaffolds—a review, J. Mater. Chem. 21 (26) (2011) 9419–9453.
[6] E. Vatankhah, et al., Artificial neural network for modeling the elastic modulus of electrospun polycaprolactone/gelatin scaffolds, Acta Biomater. 10 (2) (2014) 709–721.
[7] F. Croisier, et al., Mechanical testing of electrospun PCL fibers, Acta Biomater. 8 (1) (2012) 218–224.
[8] L. Can-Herrera, et al., Morphological and mechanical properties of electrospun polycaprolactone scaffolds: effect of applied voltage, Polymers 13 (4) (2021) 662.
[9] A.A. Conte, et al., Effects of fiber density and strain rate on the mechanical properties of electrospun polycaprolactone nanofiber mats, Front. Chem. 8 (2020) 610.
[10] R.R. Duling, et al., Mechanical characterization of electrospun polycaprolactone (PCL): a potential scaffold for tissue engineering, J. Biomech. Eng. 130 (1) (2008).
[11] K. Polak-Kraśna, et al., Parametric finite element model and mechanical characterisation of electrospun materials for biomedical applications, Materials 14 (2) (2021) 278.
[12] D. Mondal, M. Griffith, S.S. Venkatraman, Polycaprolactone-based biomaterials for tissue engineering and drug delivery: current scenario and challenges, Int. J. Polym. Mater. Polymeric Biomater. 65 (5) (2016) 255–265.
[13] R. Augustine, et al., Dose-dependent effects of gamma irradiation on the materials properties and cell proliferation of electrospun polycaprolactone tissue engineering scaffolds, Int. J. Polym. Mater. Polymeric Biomater. 64 (10) (2015) 526–533.
[14] E. Cottam, et al., Effect of sterilisation by gamma irradiation on the ability of polycaprolactone (PCL) to act as a scaffold material, Med. Eng. Phys. 31 (2) (2009) 221–226.
[15] Z. Asvar, et al., Evaluation of electrospinning parameters on the tensile strength and suture retention strength of polycaprolactone nanofibrous scaffolds through surface response methodology, J. Mech. Behav. Biomed. Mater. 75 (2017) 369–378.
[16] T. Khatti, H. Naderi-Manesh, S.M. Kalantar, Application of ANN and RSM techniques for modeling electrospinning process of polycaprolactone, Neural Comput. Appl. 31 (1) (2019) 239–248.
[17] A. Anindyajati, P. Boughton, A.J. Ruys, Modelling and optimization of polycaprolactone ultrafine-fibres electrospinning process using response surface methodology, Materials 11 (3) (2018) 441.
[18] D.J. Thomas, D. Singh, 3D Printing in Medicine and Surgery: Applications in Healthcare, Woodhead Publishing, 2020.
[19] H. Zahouani, et al., Characterization of the mechanical properties of a dermal equivalent compared with human skin in vivo by indentation and static friction tests, Skin Res. Technol. 15 (1) (2009) 68–76.
[20] H. Nosrati, et al., Nanocomposite scaffolds for accelerating chronic wound healing by enhancing angiogenesis, J. Nanobiotechnol. 19 (1) (2021) 1–21.
[21] L.L. Lima, et al., Coated electrospun bioactive wound dressings: mechanical properties and ability to control lesion microenvironment, Mater. Sci. Eng. C 100 (2019) 493–504.
[22] D. de Cassan, et al., Impact of sterilization by electron beam, gamma radiation and X-rays on electrospun poly-(ε-caprolactone) fiber mats, J. Mater. Sci. Mater. Med. 30 (4) (2019) 42.
[23] L. Bosworth, A. Gibb, S. Downes, Gamma irradiation of electrospun poly (ε-caprolactone) fibers affects material properties but not cell response, J. Polym. Sci. B Polym. Phys. 50 (12) (2012) 870–876.

[24] C.F. Rediguieri, et al., Impact of sterilization methods on electrospun scaffolds for tissue engineering, Eur. Polym. J. 82 (2016) 181–195.
[25] V. Kumar, et al., Radiation Effects in Polymeric Materials, Springer, 2019.
[26] P. Bhaskar, et al., Cell response to sterilized electrospun poly (ε-caprolactone) scaffolds to aid tendon regeneration in vivo, J. Biomed. Mater. Res. 105 (2) (2017) 389–397.
[27] D.C. Montgomery, Design and Analysis of Experiments, John wiley & sons, 2017.
[28] I.M. Sobol, Global sensitivity indices for nonlinear mathematical models and their Monte Carlo estimates, Math. Comput. Simulat. 55 (1–3) (2001) 271–280.
[29] A. Saltelli, et al., Global Sensitivity Analysis: the Primer, John Wiley & Sons, 2008.
[30] E. Salehi, et al., Adsorptive desulfurization of wild naphtha using magnesium hydroxide-coated ceramic foam filters in pilot scale: process optimization and sensitivity analysis, Chem. Eng. Process.-Process Intensification 152 (2020) 107937.
[31] D. Alexeev, et al., Mechanical evaluation of electrospun poly (ε-caprolactone) single fibers, Mater. Today Commun. 24 (2020) 101211.
[32] S.R. Baker, et al., Determining the mechanical properties of electrospun poly-ε-caprolactone (PCL) nanofibers using AFM and a novel fiber anchoring technique, Mater. Sci. Eng. C 59 (2016) 203–212.
[33] A. Repanas, et al., Coaxial electrospinning as a process to engineer biodegradable polymeric scaffolds as drug delivery systems for anti-inflammatory and anti-thrombotic pharmaceutical agents, Clin. Exp. Pharmacol. 5 (5) (2015) 1–8.
[34] Z.-J. Chen, et al., Polycaprolactone electrospun nanofiber membrane with sustained chlorohexidine release capability against oral pathogens, J. Funct. Biomater. 13 (4) (2022) 280.
[35] V. Komolprasert, et al., Volatile and non-volatile compounds in irradiated semi-rigid crystalline poly (ethylene terephthalate) polymers, Food Addit. Contam. 18 (1) (2001) 89–101.
[36] R. Augustine, et al., Electrospun polycaprolactone/ZnO nanocomposite membranes as biomaterials with antibacterial and cell adhesion properties, J. Polym. Res. 21 (3) (2014) 1–17.
[37] D. Sinha, et al., Gamma-induced modifications of polycarbonate polymer, Radiat. Eff. Defect Solid 159 (10) (2004) 587–595.
[38] S. Prajapati, et al., Effect of gamma irradiation on shape memory, thermal and mechanical properties of polycaprolactone, Radiat. Phys. Chem. (2022) 110671.
[39] P. Ducheyne, Comprehensive Biomaterials, vol. 1, Elsevier, 2015.
[40] A.T. Naikwadi, et al., Gamma radiation processed polymeric materials for high performance applications: a review, Front. Chem. 10 (2022).